文章编号：1001-9014(2022)06-0958-07

DOI:10.11972/j.issn.1001-9014.2022.06.003

Design considerations to increase the power-efficiency of a supper-large-optical-cavity waveguide structure diode laser

ZHOU Kun[1,2], HE Lin-An[1,2], LI Yi[1,2], HE Yu-Wen[1,2], DU Wei-Chuan[1,2*], LIU Sheng-Zhe[1,2], ZHANG Liang[1,2], HU Yao[1,2], SONG Liang[1,2], GAO Song-Xin[1,2], TANG Chun[1,2]

(1. Institute of Applied Electronics, CAEP, Mianyang 621900, China;
2. Key Laboratory of Science and Technology on High Energy Lasers, CAEP, Mianyang 621900, China)

Abstract: The considerations in the epitaxial and longitudinal design of a supper-large-optical-cavity structure diode laser in the 976-nm band are numerically studied and presented here. Mode control layers were designed underneath and up the quantum well layer to suppress the lasing of high-order transverse modes. The electron leakage was suppressed by a band energy engineering, where the electron barrier increases from the p-waveguide layer to the p-cladding layer. The optimized structure has an internal loss of 0.66 cm^{-1}, an internal quantum efficiency of 0.954, and a full width at half maximum vertical far-field angle of 17.4°. For the resonant cavity design, a liner current profile along the cavity was proposed to reduce the longitudinal spatial hole burning effect, where a power penalty of 1.0 W at 20 A is suppressed. The 4-mm-long and 100 μm wide broad-area single emitter with the supper-large-optical-cavity epitaxial structure was designed to have a high power-efficiency of about 71% at an output power of 21 W under continuous current injection at 25°C.

Key words: quantum-well lasers, supper-large-optical-cavity, carrier leakage, efficiency

提高超大光腔波导结构半导体激光器功率效率的设计考虑

周 坤[1,2], 何林安[1,2], 李 弋[1,2], 贺钰雯[1,2], 杜维川[1,2*], 刘晟哲[1,2], 张 亮[1,2], 胡 耀[1,2], 宋 梁[1,2], 高松信[1,2], 唐 淳[1,2]

(1. 中国工程物理研究院应用电子学研究所, 四川 绵阳 621900;
2. 中国工程物理研究院高能激光重点实验室, 四川 绵阳 621900)

摘要: 对976 nm波段超大光学腔结构半导体激光器的外延和谐振腔设计进行了数值研究。在量子阱层的下方和上方设计了模式控制层,以抑制快轴高阶模的激射。通过能带结构的调控抑制了电子泄漏,调控使得电子势垒从p波导层到p包层增加。优化后的外延结构内部损耗为0.66 cm^{-1},内部量子效率为0.954,远场发散角半高全宽为17.4°。对于谐振腔设计,提出了沿谐振腔线性电流分布结构,以减少空间烧孔效应,这使激光器在20 A时功率提高了1.0 W。采用超大光学腔外延结构的4 mm腔长、100 μm发光区宽度的单管芯片,在25°C连续电流注入下,21 W输出功率时达到约71%的高功率效率。

关 键 词: 量子阱激光器;超大光腔;载流子泄露;效率

中图分类号: O43　　**文献标识码**: A

Introduction

High-power broad-area (BA) diode lasers have found a wide range of industrial, medical, scientific, space and military applications [1]. In the 976-nm region, much attention has been attracted as pump sources

Received date: 2022-02-21, **revised date**: 2022-09-02　　**收稿日期**: 2022-02-21, **修回日期**: 2022-09-02

Foundation items: Supported by National Natural Science Foundation of China (11804322), the Innovation and Development Fund of CAEP (C-2020-CX2019035)

Biography: ZHOU Kun (1987-), male, Bazhong China, Ph. D. Research area involves Semiconductor laser materials and diode devices
E-mail: 17764988391@163.com.

* **Corresponding author**: E-mail: weichuandu@126.com

for erbium-fiber amplifiers, optical data storage and displays [2-4]. A supper-large-optical-cavity (SLOC) waveguide structure [5] has the benefit of lower power density on the facet [6], lower vertical far-field angle, and lower internal loss, thus high-power, high-efficiency and high reliability diode lasers. Furthermore, the lateral beam quality can be greatly improved due to the low differential modal gain of the SLOC structure [7].

However, the number of higher-order modes increases with the vertical waveguide thickness. Higher-order transverse modes in a SLOC can deteriorate the far-field characteristics [8] and reduce the power efficiency, since the lasing of higher-order modes will introduce a higher internal optical loss. Many reports focused on the design of high-power diode lasers based on the large-optical-cavity (LOC) structure [9-12], and some reports discussed the suppression of higher-order modes [12]. However, it is difficult to suppress the lasing of higher-order modes in a SLOC by changing the position of the quantum well (QW) or by the modal loss discrimination[13].

Furthermore, when a thick waveguide is adapted, electrons may accumulate around the p-waveguide, decreasing the injection efficiency of the carriers, which is the main cause of a lower electro-optical efficiency in a SLOC structure device [10-11]. B. S. Ryvkin[10] found that the broadening of the waveguide leads to a drastic reduction in the internal quantum efficiency due to the increased carrier density in the p-waveguide. Efforts were taken to overcome the decreasing of internal efficiency in the SLOC structure. Pietrzak *et al*. [14] reported an 8.6 μm thick SLOC with the vertical far-field of 15° and internal loss of 0.68 cm^{-1} with an injection efficiency of 0.70. Hasler *et al*. [15] obtained an injection efficiency of 0.91 and internal loss of 0.56 cm^{-1} using a 2.8 μm SLOC, but the vertical divergence is 50.8°. Andre. M [16-17] obtained an internal efficiency of 0.99 and internal losses of 0.8 cm^{-1} with a vertical far-field angle of 14.4° at full width at half maximum (FWHM).

The output power is also limited by mechanisms such as longitudinal spatial hole burning (LSHB) [18], which has been experimentally proved through the non-pinning of the carriers and spontaneous emission above lasing threshold in both GaAs-based[19-20] and InP-based[21] diode lasers. Narrow-stripe InP lasers showed around 25% improvement of rollover power using flared designs attributed to reduction of the LSHB effect [21]. There have been theoretical studies [22] showing the effect of LSHB on the output power in GaAs-based laser diodes. Reducing the cavity length can suppress the LSHB effect but the increase of thermal resistance degrades the output power at high injected currents. R. B. Swertfeger[23] recently found that higher current densities (and hence higher local recombination rates and higher losses) arise near the front facet due to spatial hole burning and that the non-uniformity is strongly affected by laser geometry, which is more severe for longer resonators and less severe for higher front facet reflectivity. Abdullah D. [24] reported an unfolded cavity, where the reflectivity of the rear and front facets were set equivalent with R=10%, to decrease the LSHB effect. It was reported that the unfolded cavity decreases the LSHB penalty by 10 times. However, the coupling or shaping of the laser beam might be complicated since the unfolded cavity has two equivalent output facets.

The goal of this paper is to design a SLOC structure diode laser with low vertical divergence angle and high power-efficiency. The refractive index, band energy, and thickness of the epitaxial layers were carefully optimized to effectively suppress the lasing of higher-order modes and carrier leakage. Taking into account the LSHB effect, the carrier density, gain profile and power along the cavity were calculated and analyzed based on the diode laser rate equations. The 4-mm-long and 100 μm wide broad-area single emitter with the SLOC waveguide structure was designed to obtain a high power-efficiency of about 71% at an output power of 21 W.

1 Calculation method

For the vertical waveguide simulation, the band, carrier concentration, gain, index profile, mode intensity, confinement factor, mode power, voltage, external efficiency, and far-field patterns were calculated. The 2D laser diode model was built with infinite lateral boundary condition. The cross sections due to the absorption by free electrons and holes in the materials were set to α_n=4×10^{17} cm^2 and α_p=12×10^{17} cm^2, respectively [5]. The calculation of the LSHB effect was based on the carrier and photon rate equations with the basic material and device parameters obtained from the results. The cavity length and emitter width were set to 4 mm and 100 μm in all the calculations. In the vertical waveguide model, the calculations were done under fixed lattice temperatures, while in the longitudinal calculations thermal heating effect was considered with a thermal resistance of 2.0 K/W, which is a typical value with p-down package on submount[5].

2 Vertical structure design

2.1 Reference structure

The vertical structure starts from a reference structure as shown in Table 1 The total wavegueide thickness is 3 500 nm with asymmetric n-type and p-type cladding layers. The single QW is set at the vertical position of around 4 000 nm with a p-waveguide thickness of 1 500

Table 1 Reference structure
表1 参考结构

Layer	Material	Thickness/nm	Doping
p++-contact	GaAs	200	C:2E19
p-cladding	$Al_{0.6}Ga_{0.4}As$	400	C:2E18
p-waveguide	$Al_{0.15}Ga_{0.85}As$	1 500	C:1E17
QW	$In_{0.2}Ga_{0.8}As$	8.6	undoped
n-waveguide	$Al_{0.15}Ga_{0.85}As$	1 600	undoped
n-waveguide	$Al_{0.15}Ga_{0.85}As$	400	Si:5E17
n-cladding	$Al_{0.25}Ga_{0.75}As$	1 500	Si:2E18 graded to 5E17
n-buffer	GaAs	500	Si:2E18

nm, where the confinement factor of mode0 is higher than all the higher-order modes, to ensure single transverse mode lasing [25]. The confinement factors of mode0, mode1 and mode2 are 0.43%, 0.10% and 0.08%, respectively. However, the relative thick p-waveguide leads to strong electron leakage, with a maximum concentration of about 4×10^{17} cm^{-3} as Fig. 1(b) shows. It is obvious that the leakage will decrease the carrier injection efficiency and increase the optical loss due to free carrier absorption. The leakage can be suppressed by increasing the p-type doping level, as shown in Fig. 1(b). A p-type doping concentration of 4×10^{17} cm^{-3} reduces the maximum electron concentration to about 1×10^{16} cm^{-3}. However, high-level p-type doping in the waveguide introduces large optical loss which degrades the power efficiency as the data decipited in Fig. 2.

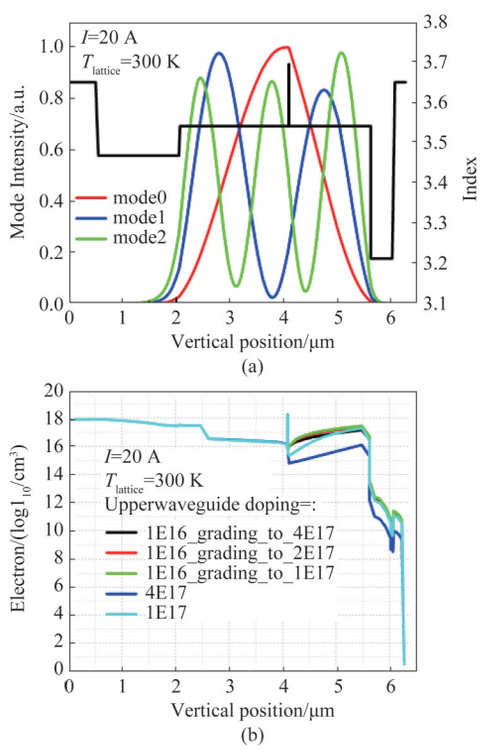

Fig.1 Transverse modes (a) and electron leakage (b) in the reference structure
图1 参考外延结构的快轴模式(a)和电子泄露(b)

2.2 Mode control

A decreased thickness of the p-waveguide can suppress the carrier leakage but high-order mode will lase. Mode control layers were designed underneath and up the QW layer to maintain a fundamental mode with thinner p-waveguide [26]. As shown in Fig. 3, 50 nm $Al_{0.08}Ga_{0.92}As$ layers were designed as the mode control layers, with which the thickness of the p-waveguide can be reduced to about 900 nm. The confinement factors of mode 0, mode1 and mode2 are 0.69%, 0.22% and 0.08%, respectively. However, high-order modes can lase if the p-waveguide thickness was further reduced according to the calculations.

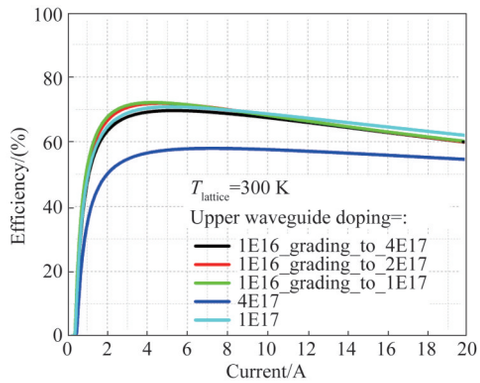

Fig. 2 Power efficiency of the reference structure with different p-waveguide doping
图2 参考外延结构激光器在不同P型波导掺杂时的功率效率

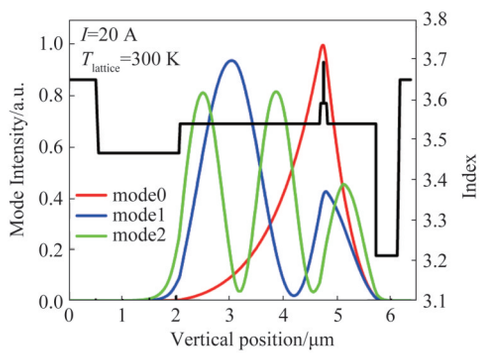

Fig. 3 Transverse modes in the SLOC with mode control layers
图3 采用了模式控制层的超大光学腔模式分布

2.3 Suppression of carrier leakage by grading waveguide

The carrier leakage can be further suppressed by a grading p-waveguide which increases the potential energy of the electrons, as the structure shown in Table 2. As plotted in Fig. 4(a), the Al content grades from 0.15 to 0.6 in the p-waveguide within a thickness of 600 nm. Single transverse mode lasing is achieved, where the confinement factors of mode0, mode1 and mode2 are 0.52%, 0.39% and 0.28%, respectively. The electron concentration in the grading and without grading p-waveguide structure were compared and plotted in Fig. 4(b). The electron concentration was reduced to 5×10^{15} cm^{-3} at 20 A, about two orders lower compared to 4×10^{17} cm^{-3} in the reference structure.

The suppression of electron leakage in the p-waveguide improves the slope efficiency, especially in the current range of above 4 A, as shown in Fig. 5(a). The slope efficiency decreases from 1.095 W/A around 1 A to 0.886 W/A around 20 A in the reference structure, while it is 1.100 W/A to 1.039 W/A in the grading structure. From the slope efficiency, an internal quantum efficiency of 0.954 at 1 A and 0.917 at 20 A can be deduced. Since the mode overlap with the p-doped layers is reduced in the grading structure, the doping level of the grading p-waveguide layer can be designed much higher. As shown in Table 2, a graded doping profile from 2×10^{17} cm^{-3} to 2×10^{18} cm^{-3} is used in the grading p-waveguide lay-

Table 2 Grading structure
表2 渐变结构

Layer	Material	Thickness/nm	Doping
p++-contact	GaAs	200	C:2E19
p-cladding	$Al_{0.6}Ga_{0.4}As$	200	C:2E18
p-waveguide	$Al_{0.15}Ga_{0.85}As$ graded to $Al_{0.6}Ga_{0.4}As$	600	C: 2E17graded to 2E18
p-waveguide	$Al_{0.15}Ga_{0.85}As$	300	C:2E17
mode control	$Al_{0.08}Ga_{0.92}As$	50	Undoped
QW	$In_{0.2}Ga_{0.8}As$	8.6	Undoped
mode control	$Al_{0.08}Ga_{0.92}As$	50	Undoped
n-waveguide	$Al_{0.15}Ga_{0.85}As$	1 600	Undoped
n-waveguide	$Al_{0.15}Ga_{0.85}As$	1 000	Si:5E17
n-cladding	$Al_{0.25}Ga_{0.75}As$	1 500	Si:2E18 graded to 5E17
n-buffer	GaAs	500	Si:2E18

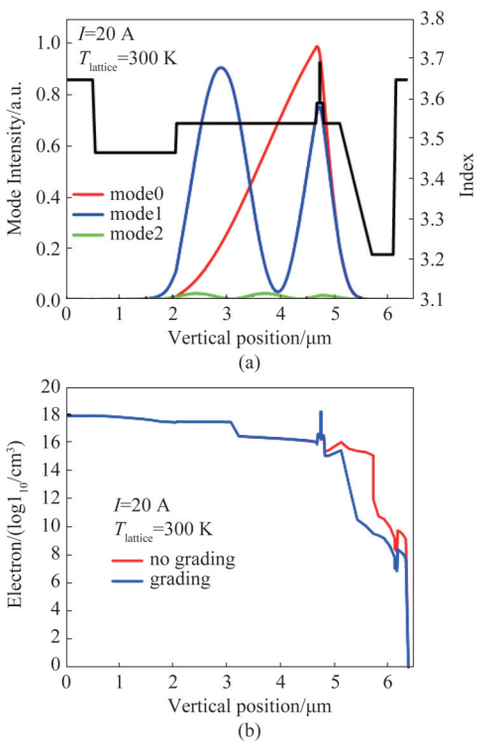

Fig. 4 (a) Transverse modes in the SLOC with grading p- waveguide, (b) electron concentration comparision with and without grading-waveguide
图4 (a) 采用了渐变P波导层的超大光学腔模式分布,(b) P波导层有渐变和无渐变时电子浓度的对比

er, which reduces the voltage by 0.142 V at 20 A compared to the reference structure as decipited in Fig. 5 (b). The power efficiency is thus improved from 61% to 71.6% at 20 A as plotted in Fig. 6(a), due to the improvement of output power and the decrease of voltage. The vertical far-field pattern is plotted in Fig. 6(b). The full width at half maximum (FWHM) vertical far-field angle is about 17.4° for both structures.

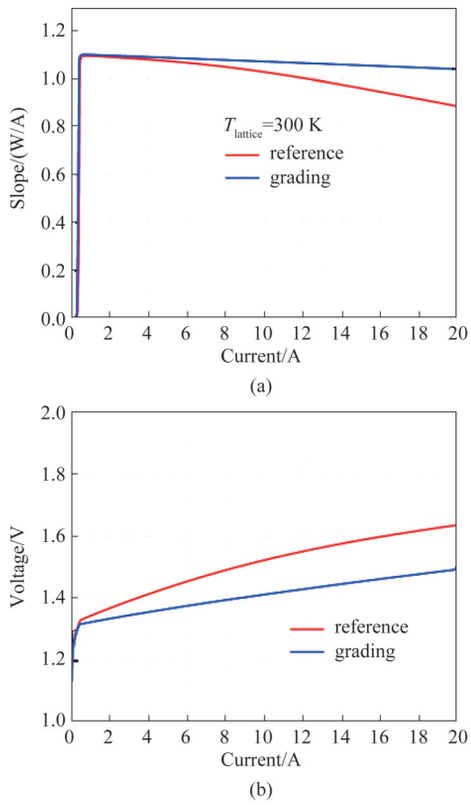

Fig. 5 Slope efficiency (a) and voltage (b) comparison of the grading and reference structures
图5 渐变P波导层激光器的斜率效率(a)和电压(b)与参考结构的对比

2.4 Characteristic temperature

Typically, the junction temperature of the laser diode will increase with the injected current. The temperature dependence of threshold, I_{th}, and slope efficiency S, are calculated as a function of lattice temperature T, using the simple empirical expressions with

$$I_{th}(T) = I_{ref}\exp\left(\frac{T}{T_0}\right), \quad (1)$$

and

$$S(T) = S_{ref}\exp\left(-\frac{T}{T_1}\right), \quad (2)$$

where T_0=300 K, I_{ref} and S_{ref} is the threshold current and slope efficiency at 300 K, respectively. In the temperature range of 300 K to 360 K, the extracted T_0 values are 174 K and 194 K for the reference and grading structure with relatively small difference. However, the extracted T_1 values are 228 K and 483K for the reference and grading structure. The improved T_1 value in the grading structure results from the suppression of carrier leakage.

Table 3 summarized the main parameters of the reference and grading structures. The key point is that the increase of modal loss and the decrease of internal quantum efficiency were suppressed in the grading structure.

3 Longitudinal design

Rate equations for diode lasers describe the relation

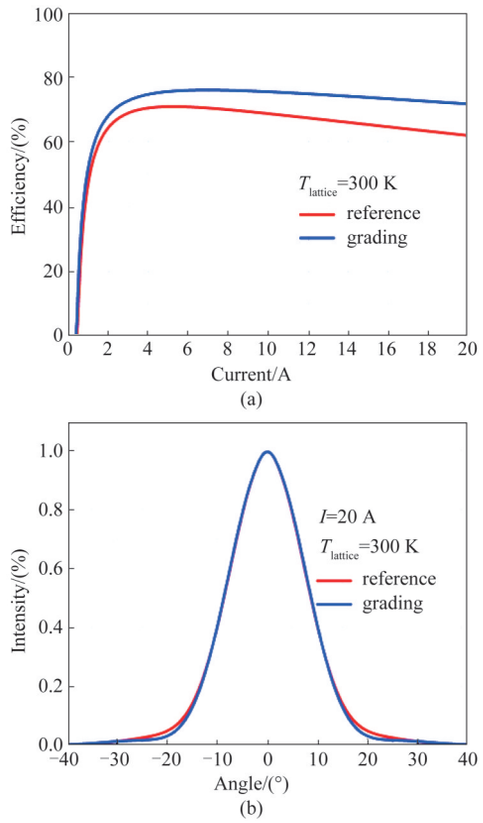

Fig. 6 Power efficiency (a) and vertical far-field (b) of the grading and reference structures
图6 渐变P波导层激光器的功率效率(a)和快轴发散角(b)与参考结构的对比

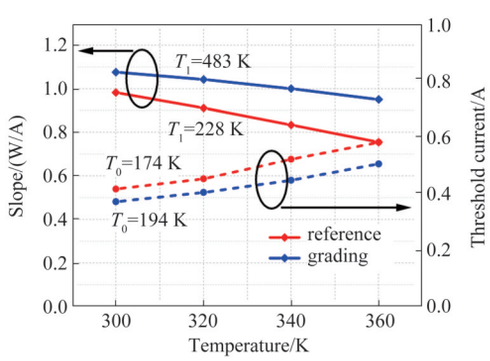

Fig. 7 Calculated temperature dependence of slope efficiency and threshold comparison of the grading and reference structures, the slope efficiency values are extracted from the output power at 10 A to 20 A
图7 计算的渐变P波导层激光器温度特性与参考结构的对比,斜率效率数值依据10 A到20 A的功率数据计算

of the density of photons and carriers (electrons) with injection current and optical gain. General rate equations assume uniform longitudinal photon density, carrier density and optical gain. However, under the effect of LSHB, rate equations must be modified [27], with local carrier density $N(z)$, local photon density $N_p(z)$, and local gain $g(z)$ varying with longitudinal position z. The detailed calculation processes of the power, gain and carrier profile was referenced from Ting Hao [28], with the material and device parameters in Table 4.

Table 3 Parameters comparison of the reference and grading structures at 300 K
表3 参考结构和渐变结构在300 K时的参数对比

Parameters	Reference	Grading
Modal loss at 1 A	0.494 cm^{-1}	0.554 cm^{-1}
Modal loss at 20 A	0.846 cm^{-1}	0.668 cm^{-1}
Internal efficiency at 1 A	0.946	0.954
Internal efficiency at 20 A	0.804	0.917
Confinement factor of QW	0.432%	0.517%
Characteristic temperature T_0	174 K	194 K
Characteristic temperature T_1	228 K	483 K
Power at 20 A	20.3 W	21.42 W
Voltage at 20 A	1.642 V	1.495 V
Efficiency at 20 A	~61%	~71.6%

Table 4 Material and device parameters for the modeling lasers
表4 激光器模型中的材料和器件参数

Cavity length /μm	4 000	Internal quantum efficiency η_i	0.954
QW thickness /nm	8.6	Optical mode Γ	0.517%
Emitter width /μm	100	Internal loss α_i/(1/cm)	0.668
HR	99%	Refractive index	3.44
AR	0.01%~30%	g_0 (1/cm)	4 000
J_{tr}/(A/cm^2)	70	Thermal resistance R_{th}/(K/W)	2.0
N_{tr}/(1/cm^3)	1.0×10^{18}	T_1/K	483
T_0/K	194	Temperature/K	300
Spontaneous coefficient B /(cm^6/s)	1×10^{-9}	Auger coefficient C/(cm^9/s)	1×10^{-30}

The output powers of the chips with and without the LSHB effect were compared in Fig. 8(a). The output power degraded with the LSHB effect with the increase of injected current. Figure 8(b) shows the power and gain profile in the chip at 20A. It is obvious that carriers accumulated on the high-reflection (HR) side because of lower optical power density. The accumulation of carriers leads to strong leakage and spontaneous emission resulting in a lower output laser power.

To suppress the LSHB effect, a linear current profile was proposed, as shown in Fig. 9(a). The current density was linearly increased from the HR facet to the anti-reflection (AR) facet, while keeping the total injected current as the same with a uniform current density. A linear current profile can be realized by a tapered electrode contact along the cavity or a patterned ohmic contact [29]. The corresponding power and gain distribution in the chips were plotted in Fig. 9(b). The gain was much lower at the HR side since the injection current density was low. The maximum modal gain reduced from

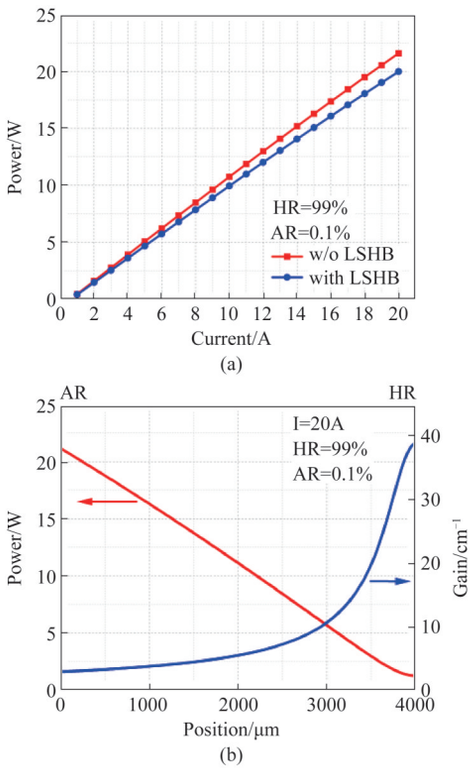

Fig. 8 Calculated power (a) and gain (b) distribution in the cavity with uniform current injection
图8 均匀注电时计算的功率(a)和增益(b)分布

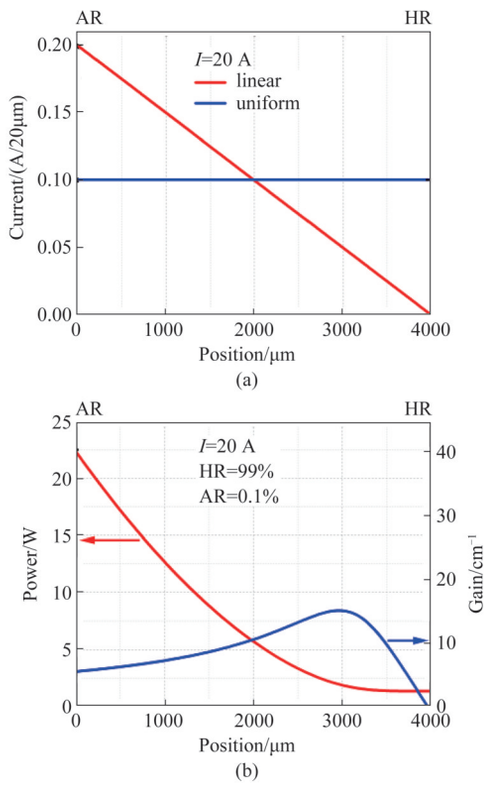

Fig. 9 Conception of linear current (a), and calculated power and gain distribution (b) in the cavity with linear current injection
图9 线性电流分布示意图(a),线性电流注入时计算的功率和增益分布(b)

39 cm^{-1} to 16 cm^{-1} compared to the uniform current injection, since the maximum carrier density was reduced from 6.4×10^{18} cm^{-3} to 2×10^{18} cm^{-3}, as shown in Fig. 10(a).

The suppression of the LSHB effect improves the output power, as plotted in Fig. 10(b). The maximum output power increased by 1.0 W at 20 A when linear current profile was used. Concerning the thermal effect with a thermal resistance of 2.0 K/W, the 4-mm-long and 100 μm wide broad-area single emitter with the SLOC waveguide structure was designed to have a high power-efficiency of about 71% at an output power of 21 W under continuous current injection at 25°C, as shown in Fig. 11.

4 Conclusions

Numerical study of the epitaxial and longitudinal design of a SLOC structure diode laser is presented in this paper. Mode control layers were used to maintain a single transverse mode with reduced p-waveguide thickness. A graded p-waveguide layer can effectively suppress the leakage of electrons and reduce the voltage. The optimized SLOC structure has an internal loss of 0.66 cm^{-1}, a confinement factor of 0.517%, an internal quantum efficiency of 0.954, a character temperature of T_0=194 K and T_1=483 K in temperature range of 300~360 K, respectively, and a full width at half maximum vertical far-field angle of 17.4°. A liner current profile along the cavity can suppress the LSHB effect, which increases the output power by 1.0 W at 20 A concerning the ther-

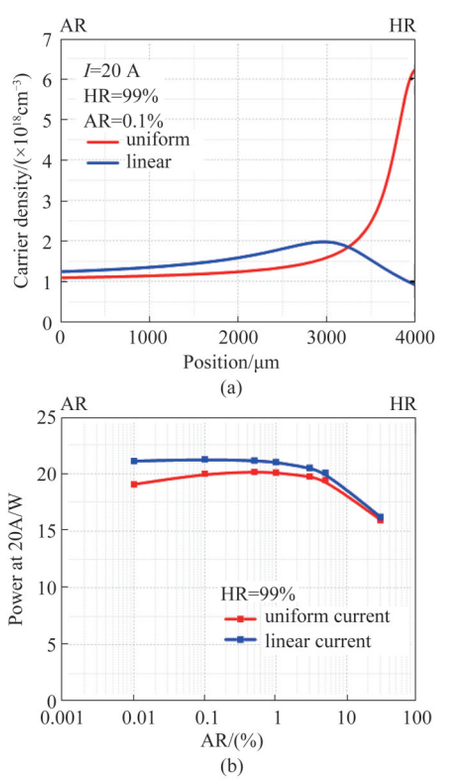

Fig. 10 Carrier density (a) and output power at 20 A (b) comparison of linear and uniform current injection
图10 计算的线性电流注入和均匀电流注入时载流子浓度(a)和20 A时输出功率(b)对比

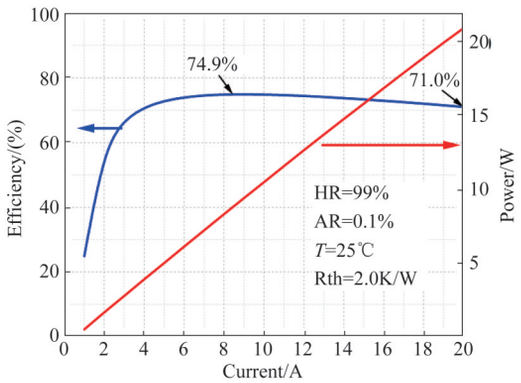

Fig. 11 Designed output power and efficiency of the 4-mm-long and 100 μm wide broad-area laser diode
图11 设计的腔长4 mm、发光区宽度100 μm的宽条型激光器输出功率和效率

mal effect with a thermal resistance of 2.0 K/W. As a result, 4-mm-long and 100 μm wide broad-area single emitter with the SLOC waveguide structure was designed to have a high power-efficiency of about 71% at an output power of 21 W under continuous current injection at 25 °C.

References

[1] Diehl R. High-power diode lasers. Fundamentals, technology, applications: With contributions by numerous experts [J]. *Topics in Applied Physics*, 2000, **8**(7):69.

[2] Jedrzejczyk D, Asbahr P, Pulka M, *et al*. High-power single-mode fiber coupling of a laterally tapered single-frequency diode laser [J]. *IEEE Photonics Technology Letters*, 2014, **26**(8):845-847.

[3] Feng F, Page H, Penty R V, *et al*. Free space optical wireless communications using directly modulated two-electrode high brightness tapered laser diode [J]. *Electronics Letters*, 2012, **48**(5):281-283.

[4] Jensen O B, Petersen P M. Single-frequency blue light generation by single-pass sum-frequency generation in a coupled ring cavity tapered laser [J]. *Applied Physics Letters*, 2013, **103**(14):141107.

[5] Crump P, Blume G, Paschke K, *et al*. 20 W continuous wave reliable operation of 980nm broad-area single emitter diode lasers with an aperture of 96μm [J]. *High-Power Diode Laser Technology and Applications VII. SPIE*, 2009, **7198**: 315-323.

[6] Wilkens M, Wenzel H, Fricke J, *et al*. High-efficiency broad-ridge waveguide lasers [J]. *IEEE Photonics Technology Letters*, 2018, **30**(6):545-548.

[7] Mikulla M, Chazan P. High-brightness tapered semiconductor laser oscillators and amplifiers with low-modal gain epilayer-structures [J]. *IEEE Photonics Technology Letters*, 1998, **10**(5):654-656.

[8] Gordeev N Y, Payusov A S, Shernyakov Y M, *et al*. Transverse single-mode edge-emitting lasers based on coupled waveguides [J]. *Optics Letters*, 2015, **40**(9):2150-2.

[9] Botez D. Design considerations and analytical approximations for high continuous-wave power, broad-waveguide diode lasers [J]. *Applied Physics Letters*, 1999, **74**(21):3102-3104.

[10] Ryvkin B S, Avrutin E A. Effect of carrier loss through waveguide layer recombination on the internal quantum efficiency in large-optical-cavity laser diodes [J]. *Journal of Applied Physics*, 2005, **97**(11):113106-113106.

[11] Ryvkin B, Avrutin E. Non-uniform carrier accumulation in optical confinement layer as ultimate power limitation in ultra-high-power broad-waveguide pulsed InGaAs/GaAs/AlGaAs laser diodes [J]. *Electronics Letters*, 2006, **42**(22):1283-1284.

[12] Pikhtin N A, Slipchenko S O, Sokolova Z N, *et al*. 16W continuous-wave output power from 100 m-aperture laser with quantum well asymmetric heterostructure [J]. *Electronics Letters*, 2004, **40**(22): 1413-1414.

[13] Tijero J M G, Odriozola H, Borruel L, *et al*. Enhanced brightness of tapered laser diodes based on an asymmetric epitaxial design [J]. *IEEE Photonics Technology Letters*, 2007, **19**(20):1640-1642.

[14] Pietrzak A, Crump P, Wenzel H, *et al*. Combination of low-index quantum barrier and super large optical cavity designs for ultranarrow vertical far-fields from high-power broad-area lasers [J]. *IEEE Journal of Selected Topics in Quantum Electronics*, 2011, **17**(6):1715-1722.

[15] Hasler K H, Wenzel H, Crump P, *et al*. Comparative theoretical and experimental studies of two designs of high-power diode lasers [J]. *Semiconductor Science & Technology*, 2014, **29** (4): 45010-45015(6).

[16] Bugge, Frank, Erbert, et al. DBR tapered diode laser with 12.7 W output power and nearly diffraction-limited, narrowband emission at 1030 nm [J]. *Applied physics, B. Lasers and optics*, 2016, B122 (4):87.1.

[17] Muller A, Zink C, Fricke J, *et al*. Efficient, high brightness 1030 nm dbr tapered diode lasers with optimized lateral layout [J]. *IEEE Journal of Selected Topics in Quantum Electronics*, 2017, **23**(6): 1-1.

[18] Chen Z, Ling B, Bai J, *et al*. Performance limitation and mitigation of longitudinal spatial hole burning in high-power diode lasers [J]. *Proceedings of Spie the International Society for Optical Engineering*, 2012, **8277**:245-252.

[19] Bennett A J, Clayton R D, Xu J M. Above-threshold longitudinal profiling of carrier nonpinning and spatial modulation in asymmetric cavity lasers [J]. *Journal of Applied Physics*, 1998, **83**(7):3784-3788.

[20] Hao T, Song J, Liptak R, *et al*. Experimental verification of longitudinal spatial hole burning in high-power diode lasers [J]. *SPIE*, 2014, **9081**:117-125.

[21] Guermache A, Voiriot V, Locatelli D, *et al*. Experimental demonstration of spatial hole burning reduction leading to 1480-nm pump lasers output power improvement [J]. *IEEE Photonics Technology Letters*, 2005, **17**(10):2023-2025.

[22] Wenzel H. Basic aspects of high-power semiconductor laser simulation [J]. *IEEE Journal of Selected Topics in Quantum Electronics*, 2013, **19**(5):1-13.

[23] Swertfeger R B, Patra S K, Deri R J, *et al*. Longitudinal current crowding as power limit in high power 975 nm diode lasers [C]. 2020 IEEE Photonics Conference (IPC). IEEE, 2020:1-2.

[24] Demir A, Peters M, Duesterberg R, *et al*. 29.5W continuous wave output from 100 μm wide laser diode [J]. *SPIE*, 2015, **9348**: 129-134.

[25] Zhou K, Du W, Li Y, *et al*. Suppression of higher-order modes in a large-optical-cavity waveguide structure for high-power high-efficiency 976-nm diode lasers [J]. *Superlattices and Microstructures*, 2019, **129**:40-46.

[26] Crump P, Pietrzak A, Bugge F, *et al*. 975 nm high power diode lasers with high efficiency and narrow vertical far field enabled by low index quantum barriers [J]. *Applied Physics Letters*, 2010, **96**(13): 719803.

[27] Avrutin E A, Ryvkin B S. Effect of spatial hole burning on output characteristics of high power edge emitting semiconductor lasers: A universal analytical estimate and numerical analysis [J]. *Journal of Applied Physics*, 2019, **125**(2):023108.1-023108.8.

[28] Hao T, Song J, Leisher P O. Rate equation analysis of longitudinal spatial hole burning in high-power semiconductor lasers [J]. *SPIE*, 2014, **9134**:155-161.

[29] Wang L J, Tong C Z, Shu S L, *et al*. Loss tailoring of high-power broad-area diode lasers. [J]. *Optics letters*, 2019, **44**(14):3562-3565.